

Inhomogeneity in Spectral Transmission of the Coated *UBVRI* Filters of BFOSC and its Influence on Photometry

Bao-An Yao^{1*} and Lin Huang²

¹ Shanghai Astronomical Observatory, Chinese Academy of Sciences, Shanghai 200030

² National Astronomical Observatories, Chinese Academy of Sciences, Beijing 100012

Received 2002 May 31; accepted 2002 August 26

Abstract In order to realize the Johnson *UBV* and Kron-Cousins *RI* photometric systems in BFOSC, glass filters were purchased according to the Bessell prescription. All the filters are anti-reflection coated on both sides to increase the transmission. By comparing two dome flat-field exposures taken through any one of these filters set in two orientations 90° apart, inhomogeneities in the filter transmission is clearly demonstrated. Using a PDS microphotometer, we have confirmed that the form of their spectral transmission curve varied from point to point on the filters. This kind of inhomogeneity cannot be eliminated by dividing by flat-fielding exposure and must be ascribed to inhomogeneities in the coating. This is not some accidental defect in coating, it is in the existing coating technique because all the filters (including the narrow-band interference ones) for the BFOSC and a H β filter made by another manufacturer showed a similar pattern. We found that for the studies of variable stars with amplitudes less than 0.05 mag. or studies aiming at establishing accurate C-M diagrams of star clusters, the usual uncoated Schott glass filters of Bessell's prescription are to be preferred.

Key words: methods: data analysis — techniques: photometric

1 INTRODUCTION

BFOSC (BAO Faint Object Spectrograph and Camera) is a precise multifunction instrument attached to the 2.16-meter telescope at the Xinglong Station of the Beijing Astronomical Observatory (BAO), now reorganized into the National Astronomical Observatories of China (NAOC). It is now equipped with 31 filters including seven broad-band ones as listed in the following table, and 24 narrow-band ones. These filters were made by Customs Scientific, USA, and all were anti-reflection coated on both sides (see Table 1).

Among the broad-band filters, the *U*, *B*, *V*, *R* and *I* are glass combinations of Bessell's prescription (Bessell 1990) for realizing the Johnson's (*UBV*) and Kron-Cousins' (*RI*) systems, and the filter *Z* is a long-pass interference filter for the wavelength range longer than 910 nm.

* E-mail: yba@center.shao.ac.cn

These six filters are used for astronomical photometry. The last one in the table, 385LP, is specially designed for removing the second order spectrum with $\lambda > 385$ nm in spectroscopy mode, and is not included in the present test.

Table 1 Broad-Band Filters Used in BFOSC

Designation	Prescription
<i>U</i>	1 mm UG1 + 1 mm BG39 + 3 mm WG305
<i>B</i>	2 mm GG385 + 1 mm BG12 + 2 mm BG39
<i>V</i>	2 mm GG495 + 3 mm BG39
<i>R</i>	2 mm OG570 + 3 mm KG3
<i>I</i>	3 mm RG9 + 2 mm BK7
<i>Z</i>	910LP
385LP	3 mm GG385

In an investigation on the photometric performance of BFOSC carried out in April-May of 1998, it was found that the transmissions of *B* and *V* filters were not homogeneous. The inhomogeneity manifested in the following. The two flat-fieldings taken with an integrating sphere (the lamp was stabilized) for either *B* or *V* filter were highly consistent with each other; and the two flat-fieldings taken under the same conditions but with the filters rotated by 90 degrees were also highly consistent with each other. However, the mean of the first two flat-fieldings divided by the mean of the last two ones showed a clear pattern of systematic inhomogeneity (not random fluctuations) amounting to about 2%. Later, all the *UBVRI* filters were checked similarly using the dome flat-fielding. For each filter, the mean of the two dome flat-fieldings taken under the same conditions was divided by the mean of other two dome flat-fieldings taken with the filter rotated by 90 degrees. The results are shown in the upper part of Fig. 1 with the corresponding contours in the lower part. The largest relative variation appears in *U* ($\approx 7\%$). For others the relative variation is about 2%–3%.

The glass of the broad-band filters was bought from Schott Company, whose products have long been used in astronomical photographic and photoelectric photometry. Within the present photometric accuracy, we have never discovered, or found in literature, that Schott glass filters ever showed such a large degree of inhomogeneity. Hence, our suspicion turned to the possible inhomogeneity in the transmission of the coatings, and decided to carry out comprehensive tests on all BFOSC filters (except 385LP, because this filter is not used for photometry and the inhomogeneity in its transmission would have no serious consequences). Although the title of this paper concerns the broad-band *UBVRI* filters, we also include the interference filters in our test because it seems that no one has touched this problem in the literature. We were quite certain that, if the inhomogeneities mentioned-above are caused by the coatings, then the interference filters, even if they are not anti-reflection-coated, would show similar inhomogeneities because the technologies used for making the interference coatings are similar to those used for making the anti-reflection coatings. Any conclusion in this respect would be of interest for anyone using interference filters in their investigations.

2 EFFECT OF INHOMOGENEITY IN FILTER TRANSMISSION

It is well known that, in order to remove the effect of inhomogeneity in sensitivity of individual CCD pixels, the reduction of the raw CCD images requires subtracting the bias and dividing by the bias-subtracted flat-fielding. Denote by $I(i, j)$ the readout of intensity at

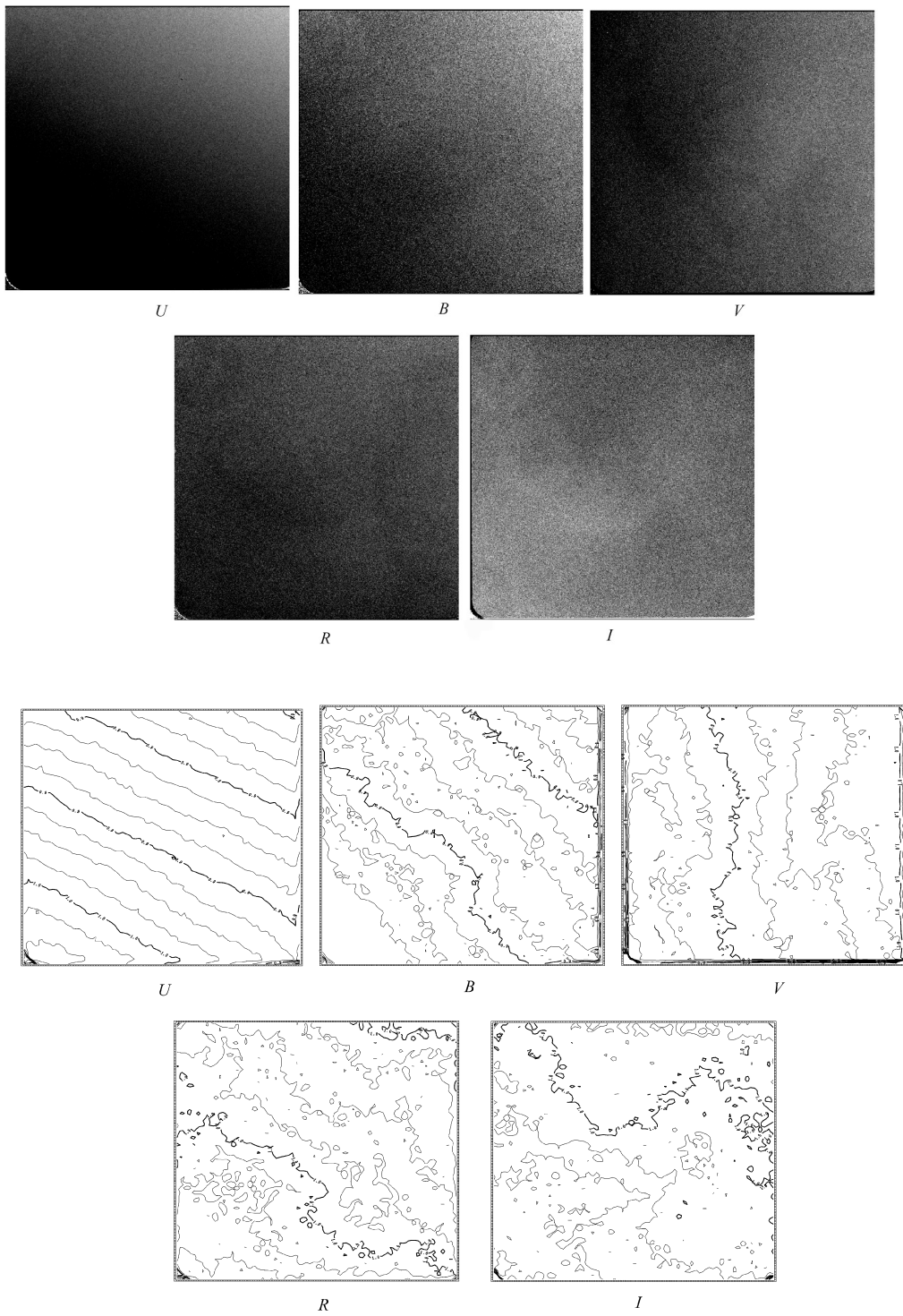


Fig. 1 Ratios of two flat-fieldings taken with the filter orientation differing by 90 degrees (upper part) and the corresponding transmission contours (lower part) for the *U*, *B*, *V*, *R* and *I* filters of BFOSC.

the pixel of i -th column and j -th row in a bias-subtracted CCD image; by $E(i, j)$ the readout of the true intensity to be found at the same pixel; by $R(i, j)$ the response function at that pixel (including reflection and absorption in optics of the telescope and BFOSC, transmission in filters, and the sensitivity of the CCD). In a flat-field image taken with an extended light source of homogeneous intensity E_0 , the readout of intensity at i -th column and j -th row is denoted by $FF(i, j)$, of course, with bias subtracted (this subtraction will not be stated every time in the following text). Then dividing by the flat-fielding results in

$$\frac{I(i, j)}{FF(i, j)} = \frac{E(i, j)R(i, j)}{E_0R(i, j)} = \frac{E(i, j)}{E_0}, \quad (1)$$

which gives the true intensity distribution, up to a constant factor, of the celestial object in the CCD image.

Strictly speaking, Eq. (1) is valid only for monochromatic light. In more detailed form, it should be

$$\frac{I(i, j, \lambda)}{FF(i, j, \lambda)} = \frac{E(i, j, \lambda)p(\lambda)r(i, j, \lambda)S(i, j, \lambda)}{E_0(\lambda)p(\lambda)r(i, j, \lambda)S(i, j, \lambda)} = \frac{E(i, j, \lambda)}{E_0(\lambda)}, \quad (2)$$

where $p(\lambda)$ is the spectral throughput of the whole optical system including the telescope and the BFOSC; $r(i, j, \lambda)$ is the spectral transmission of the filter; and $S(i, j, \lambda)$ is the spectral sensitivity of the CCD pixel.

It should be noted that if $r(i, j, \lambda) = 0$, then Eq. (2) is meaningless. This could happen when narrow-band interference filters are used. For example, in searching for H α emission objects through a narrow-band H α filter on a Schmidt telescope of powerful short focal ratio, it should be taken into account, for manufacturing the H α filter, that the central wavelength of the filter will be shifted for light that passes through the edge of the field of view and so does not fall normal to the filter. If the filter is incorrectly designed or fabricated, the central wavelength of the interference filter may differ from H α so that H α radiation cannot pass it, and the correction by flat-fielding cannot be applied. For broad-band photometry, Eq.(2) is integrated and becomes

$$\frac{I(i, j)}{FF(i, j)} = \frac{\int_{\lambda_1}^{\lambda_2} E(i, j, \lambda)p(\lambda)r(i, j, \lambda)S(i, j, \lambda)d\lambda}{\int_{\lambda_1}^{\lambda_2} E_0(\lambda)p(\lambda)r(i, j, \lambda)S(i, j, \lambda)d\lambda}. \quad (3)$$

Here λ_1 and λ_2 are respectively the lower and upper integration limits for the working wavelength region of the filter.

Generally the distribution form of $S(i, j, \lambda)$ as a function of λ changes with i and j on the CCD. Moreover, for Schott glass filters, $R(i, j, \lambda)$ should be independent of i and j , or differ only by a constant factor. The numerator in Eq. (3) is the usual definition of an instrumental photometric system.

However, $E(i, j, \lambda)$ cannot be determined from Eq. (3), and in broad-band photometry, what concerns us is the stability of the magnitude system. This requires only that the magnitudes measured from the images of a star must be the same regardless where the images appear on the CCD; however, this requirement is not satisfied in the general case.

As soon as CCD was introduced into astronomical observations, it was noted, and not just once (e.g., King, 1986) that, because of variations in $S(i, j, \lambda)$, the spectral energy distribution of the source used for flat-fielding must be the same as that of the celestial object to be measured, that is, $E_0(\lambda)$ in Eq. (3) can be written as $E_0(\lambda) = kE(i, j, \lambda)$ where k is a constant. Therefore, if the objects observed in the field covered by CCD are of the same type and differ from each

other only in their brightness, then everything is OK. In practice, however, this condition is not fulfilled, for example, when star clusters are observed. It sounds very bad, but fortunately the real results obtained so far are not so bad. In the literature, a large number of C-M diagrams of star clusters, obtained by using flat-field corrections according to Eq. (1), have been published without complaint about the above-mentioned difficulties within the allowed error limits. In addition, all the CCD standard fields including the largest sample of precise *BVRI* standards (Stetson 2000) have been obtained this way. This, in fact, implies that, within the error limits, the changes of $S(i, j, \lambda)$ with position only amount to a constant factor, that is, $S(i, j, \lambda) = K(i, j)S(\lambda)$ where $K(i, j)$ is a factor depending on i and j . Hence, Eq. (3) becomes

$$\frac{I(i, j)}{FF(i, j)} = \frac{[\int_{\lambda_1}^{\lambda_2} E(i, j, \lambda)p(\lambda)r(\lambda)S(\lambda)d\lambda]K(i, j)}{[\int_{\lambda_1}^{\lambda_2} E_0(\lambda)p(\lambda)r(\lambda)S(\lambda)d\lambda]K(i, j)} = \frac{\int_{\lambda_1}^{\lambda_2} E(i, j, \lambda)p(\lambda)r(\lambda)S(\lambda)d\lambda}{\int_{\lambda_1}^{\lambda_2} E_0(\lambda)p(\lambda)r(\lambda)S(\lambda)d\lambda}. \tag{4}$$

The effect of Eq. (4) is that the response function is independent of i and j , and is the same for the whole CCD image. In this case the flat-fielding is successful.

If, however, the spectral transmission curve of the filter also changes with the position, then an additional uncertainty appears in Eq. (3). This means that the filter would have different colors at different parts or, in other words, different parts of the filter are in fact of different types. This uncertainty, as intuition tells us, cannot be corrected by flat-fielding.

In order to show this mathematically, we modify Eq. (3) by using the theorem of mean and have

$$\begin{aligned} \frac{I(i, j)}{FF(i, j)} &= \frac{\int_{\lambda_1}^{\lambda_2} E(i, j, \lambda)p(\lambda)r(i, j, \lambda)S(i, j, \lambda)d\lambda}{\int_{\lambda_1}^{\lambda_2} E_0(\lambda)p(\lambda)r(i, j, \lambda)S(i, j, \lambda)d\lambda} \\ &= \frac{E(i, j, \lambda_0) \int_{\lambda_1}^{\lambda_2} p(\lambda)r(i, j, \lambda)S(i, j, \lambda)d\lambda}{E_0(\lambda'_0) \int_{\lambda_1}^{\lambda_2} p(\lambda)r(i, j, \lambda)S(i, j, \lambda)d\lambda} \\ &= \frac{E(i, j, \lambda_0)}{E_0(\lambda'_0)}, \end{aligned} \tag{5}$$

here, we have $\lambda_1 < \lambda_0 < \lambda_2$, $\lambda_1 < \lambda'_0 < \lambda_2$ and generally $\lambda_0 \neq \lambda'_0$.

Both λ_0 and λ'_0 are some kind of effective wavelengths. They depend not only on the spectral type of the objects observed and the spectral energy distribution of the flat-field light source, but also on the positions on the filter and the CCD. For the same star, the value of $E(i_1, j_1, \lambda_{01})/E_0(\lambda'_{01})$, measured at pixel (i_1, j_1) is usually different from the value $E(i_2, j_2, \lambda_{02})/E_0(\lambda'_{02})$, measured at another pixel (i_2, j_2) , and also $\lambda_{01} \neq \lambda_{02}$, $\lambda'_{01} \neq \lambda'_{02}$. Such an effect would increase the scatter in the observed C-M diagrams of star clusters and lead to misidentification of new variable stars of small amplitudes.

As we have mentioned before, the spectral sensitivity of CCD pixels changes with the position, but in practice the flat-field corrections made so far with Eq. (1) are useful within the limits of errors. Could the changes in the spectral transmission of BFOC filters be also ignored? Although the lessons in using the moldy filters said “No” (Yao et al. 2002), this question could be answered more strictly through calculations if the spectral transmission curves at different positions on the filter can be measured. Unfortunately, we could not find a spectral micro-photometer to perform such point-by-point measurements. What we could do was to carry out, as described in the next section, a semi-quantitative and relative test supplemented by observing a sky region containing standard stars.

3 MEASUREMENTS OF INHOMOGENEITY OF FILTERS WITH PDS

We have scanned the BFOSC filters with the PDS at Purple Mountain Observatory. It is a high precision, full-automatic micro-photometer and can measure the transmission at individual positions on the filter by scanning it point-by-point with a very fine light-beam. However, our measurements suffered the following drawbacks and limitations:

(1) Because the illuminating light source of PDS has a continuous spectrum and the detector is a blue-sensitive S-11 type photomultiplier, all the BFOSC filters transmitting only longer wavelengths absorb the shorter ones. This made it impossible to measure, for example, the I and Z broad-band filters (see the Table 1 in Introduction) and some $H\alpha$ interference filters with large enough redshifts.

(2) Narrow-band interference filters were tested also with the source of continuous spectrum. Therefore, the measured changes of the transmission do not include the effects of the shifts of central wavelengths. In other words, even if the central wavelength has shifted, this may not be discovered by the PDS.

(3) For testing the V filter, we modified the spectral energy distribution of the PDS light source by inserting successively the PDS built-in red, green and blue color glasses into the measuring light path. This is equivalent to changing the color temperature of the light source. Then the modified light beam passed through the V filter and fell on the photomultiplier. In this way we actually measured the long, middle and short wavelength parts, separately, just as is done in a low resolution spectrophotometry within the wavelength range of the V filter. We do not know the effective wavelengths and the absolute intensities of these long, middle and short wavelength parts, but we do know their relative values. This is why we describe our method as semi-quantitative and relative.

(4) As mentioned in the Introduction, the U , B , V , R and I filters showed similar inhomogeneities in the test with the BFOSC integrating sphere and dome flat-fielding. Unfortunately, of the U , B , V , R filters which can be measured with the PDS, only the V filter could be tested separately with red, green and blue glasses because the U and B filters do not transmit green and red light, and because the R filter transmits only red light.

(5) What we measured with PDS are specular densities that differ from, and cannot be reduced to, diffuse densities. However, according to the experience gained in our earlier measurements with photographic emulsions, the finer the emulsion grains, the closer are the values of the two kinds of densities. Because the filters have no grains, we reasonably expect that the measured densities are even closer to the diffuse ones than in the case of photographic emulsions.

(6) We have measured the BFOSC filters twice with the PDS. In July, 1999, the filters were fast and repeatedly scanned along two diameters perpendicular to each other, and the results were averaged. In this case, the PDS readouts divided by 800 were just the specular densities. They are in this sense absolute values. The second time, in March, 2000, because of defects in the high-voltage power supply of the PDS, the PDS could not reach its ideal focusing state. Therefore, the readouts divided by 800 were not the specular densities. In the latter case, what was important were the relative changes at individual points on the filters.

3.1 Measurements of July, 1999

Our original purpose was to scan all the filters and to calculate, whenever possible, their transmission contours. However, we soon discovered that regular stripes parallel to the scanning direction appeared in the plots with a period of about 14 minutes. It was certain that these

stripes resulted from the instability of the PDS system itself because the same stripes, in the sense of their being parallel to the scanning direction, appeared regardless of the orientation of the filter. This made it impossible to measure the contours. Instead, we carried out fast and repeated scanning along two mutually perpendicular diameters, and took their averages. The results for the V filter are shown in Fig. 2, in which the ordinate is the density multiplied by 800 and the abscissa is the sample number along the 60 mm diameter scanned. All the four scans in this figure clearly showed a monotonic change of the transmission from one end of the diameter to the other. The transmission difference at the two ends of the 60-mm diameter may amount to about 5%. Because the X and Y directions on the filter were chosen arbitrarily and did not represent the direction of maximal or minimal changes, the true maximal changes may exceed 5%. It is especially worth noting that the results of the scans made with a green and a red glass inserted in the PDS measuring path are different. For example, in Fig. 2a the left end of the curve is lower than the right end, but in Fig. 2c the left end is higher. This shows that the form of the spectral transmission curve of the V filter changes from point to point. With such a filter, the results measured for the same star may vary depending on where it falls on the CCD, and may cause troubles in the transformation of the photometric systems.

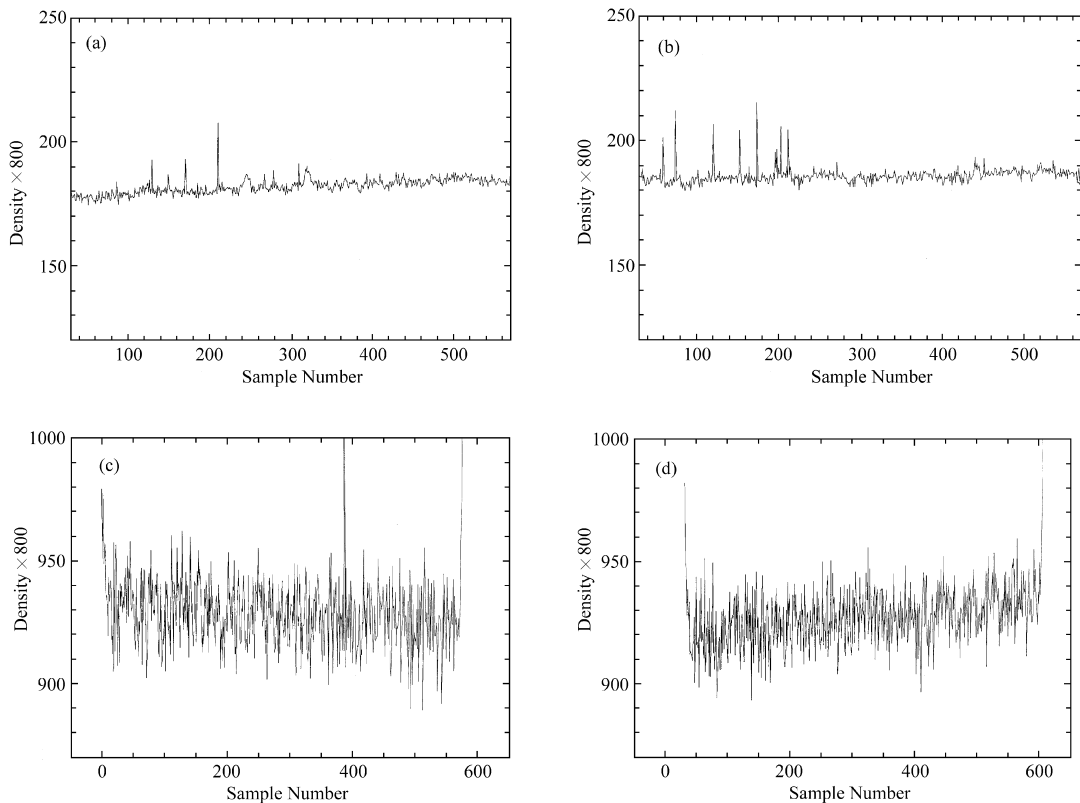


Fig. 2 Monotonic changes of transmission of V filter along a diameter.
 a. Mean of 9 fast repeated scans along X direction with green glass inserted.
 b. Mean of 10 fast repeated scans along Y direction with green glass inserted.
 c. Mean of 10 fast repeated scans along X direction with red glass inserted.
 d. Mean of 11 fast repeated scans along Y direction with red glass inserted.

Now let us estimate quantitatively the influence on practical observation caused by the monotonic changes of transmission shown in these scans. The optical system of BFOSC makes any parallel beam from the collimator pass the pupil before entering the camera. According to the distance between the pupil and the filter, we can calculate rather precisely the distance between the centers of the circles through which two parallel beams pass the filter. For the two beams corresponding to the opposite corners of the field covered by the CCD, this distance is 13.38 mm. Since the transmission changes monotonically over the field, it is reasonable to assume that the average transmission in any of the above-mentioned circles can be approximately represented by the transmission at the center of that circle. Under this assumption and taking into account the maximal rate of change of transmission along a diameter, we estimate that the relative difference between the transmissions at the two opposite corners of the CCD to be 0.013. A difference in transmission of this size would cause no serious effects in most survey programs when not considering the transformation of photometric systems. It may not, of course, be ruled out that this estimate is too optimistic because our method is semi-quantitative, and because we did not use the blue glass in the PDS measuring path. The blue, green and red glasses are also a kind of broad-band filters with their transmission curves overlapping each other for certain wavelengths. Also we could not test if the transmission changes with the incidence angle, etc.

3.2 Measurements of March, 2000

In order to increase the S/N-ratio, this time we deliberately chose the maximal scanning diaphragm of $0.4 \times 0.5 \text{ mm}^2$ and use the “white light” for all scans except those shown in Fig. 8 (see below). Figs. 3–6 are the large-scale averaged results for those filters that can be measured on the PDS. The plots were obtained by smoothing, with the Command “median” of IRAF, over a square box with sides 1/10 the filter diameter. Thanks to the fact that the light beam from a star intersects the filter in quite a big circle, the large-scale smoothing is indeed a good simulation of the real exposure (forget the inhomogeneities at the edges in the figures; they resulted from the smoothing over a square box covering an area partly outside the circle of the filter). Here we also give the results of the $H\beta$ interference filter used by BATC group (Fig. 7). This filter was coated by another US company.

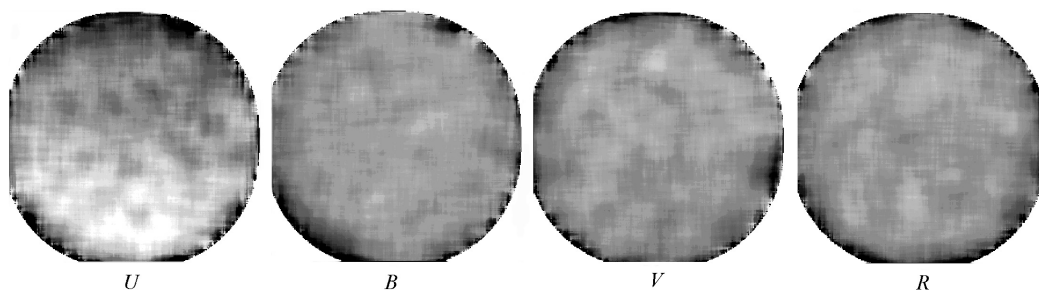


Fig. 3 Large-scale averaged scans in “white light” for the broad-band filters.

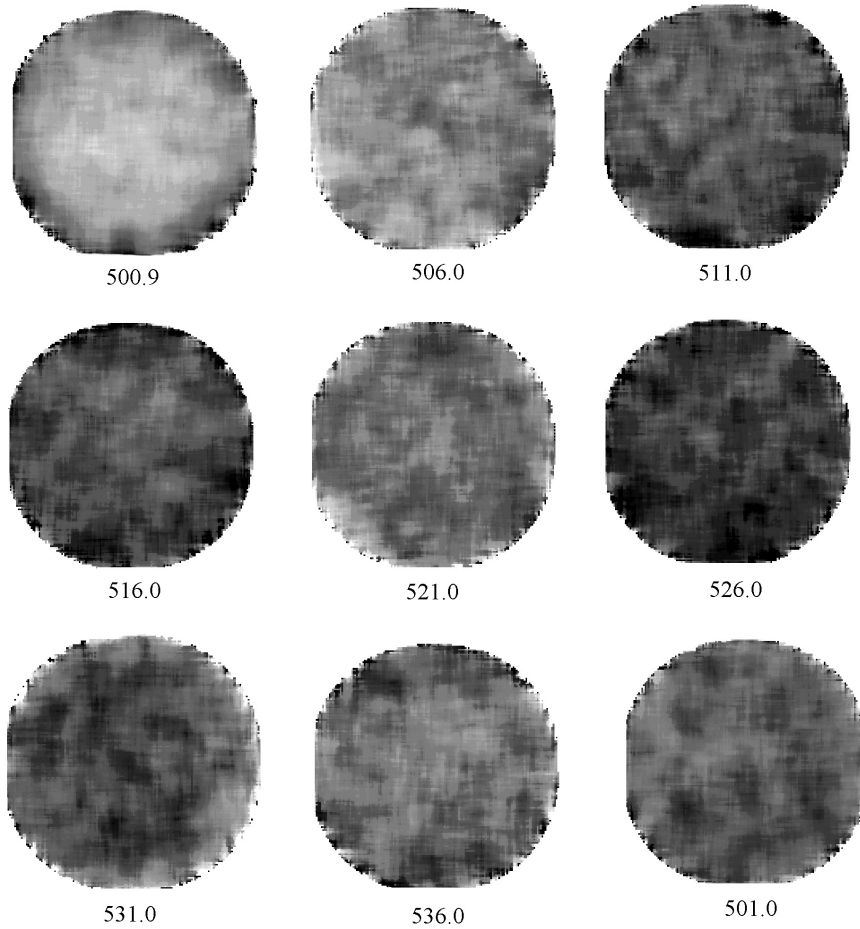


Fig. 4 Large-scale averaged scans in “white light” for the [OIII] group interference filters. The numbers are the central wavelengths in nm.

We present here the scanning results of all the measured broad-band and narrow-band interference filters to emphasise that, even if the interference filters are not anti-reflection-coated, they would show similar inhomogeneities because the modern techniques for anti-reflection and interference coating are similar, that is, the devices to be coated and the coating materials are placed in a vacuum chamber, and then by electric heating the evaporated materials are settled onto the surfaces of the rotating devices. To our best knowledge, our point-by-point scanning of filters on PDS for the first time demonstrates clearly the inhomogeneities resulting from the imperfections of the techniques. This may be a good warning to those who use interference filters in their investigations. It should be noted that this is not a particular problem with this or that manufacturer, but a common problem with the technology. Therefore, we must sadly recognize that the inhomogeneities displayed in these figures are not abnormal.

However, the key to the question is whether the form of the spectral transmission curves varies. The upper panel of Fig. 8 shows the results for the *V* filter obtained by inserting the blue, green and red glass into the PDS measuring path (for the blue glass we used the F-mode

scanning, and because of the imperfections of the F-mode, the very left part of this plot is wrong). It can be seen from these figures that the inhomogeneity patterns, the numbers, sizes, shapes and the relative intensities of the dark spots and stripes, are different in different scans. In the scanning obtained in green light, the dark spots are the most numerous. In the scanning in blue light, however, there appeared one more big spot just to the right of the center. The corresponding contours are shown in the lower panel of Fig. 8. Note that the spots and stripes are not caused by strains on the filter surface. Also note that the appearance of the V filter scanned in “white light” is different from that in blue, green or red light!! The scanning step of the former was twice as large as in the latter and hence the resolution was lower, but this could not explain their difference. Obviously, such patterns must be the manifestation of changes in the spectral transmission over the whole filter.

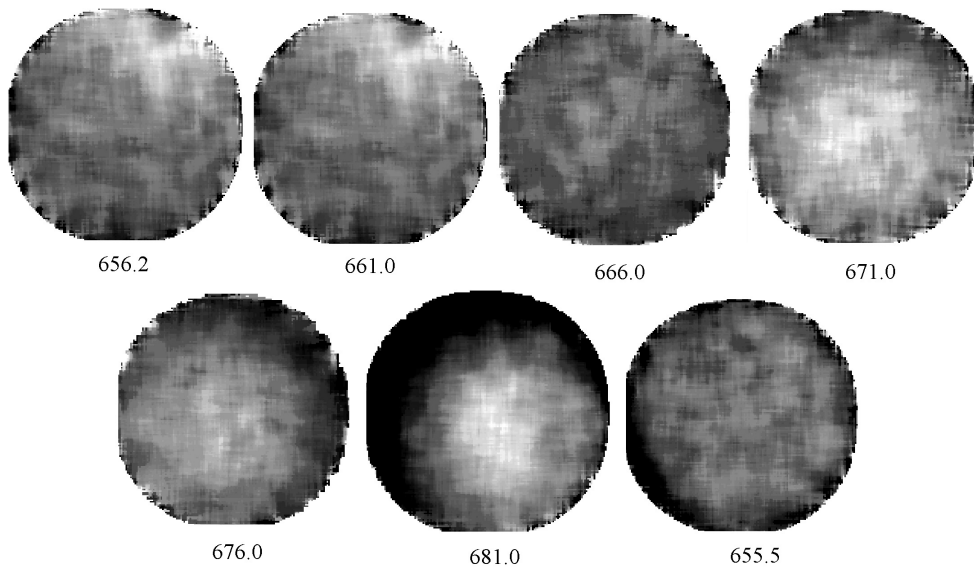


Fig. 5 Large-scale averaged scans in “white light” for the $H\alpha$ group interference filters. The numbers are the central wavelengths in nm.

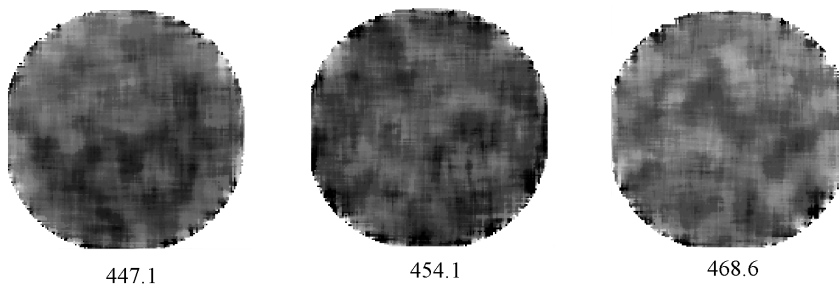


Fig. 6 Large-scale averaged scans in “white light” for the He group interference filters. The numbers are the central wavelengths in nm.

As mentioned before, we were able to do our PDS measurements in this way only for the V filter, but it would be quite improbable that such defects in the coating exist only for the V filter. Because the U , B , R and I filters showed similar features in flat-field tests (see Introduction), it would be reasonable to believe that similar changes in spectral transmission exist for all broad-band filters.

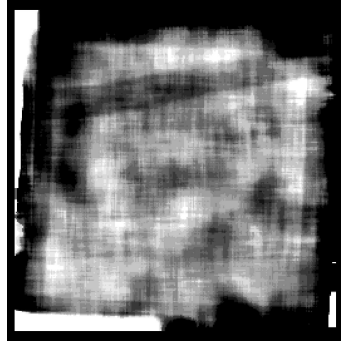


Fig. 7 Large-scale averaged scan in "white light" for the H β interference filter of BATC group.

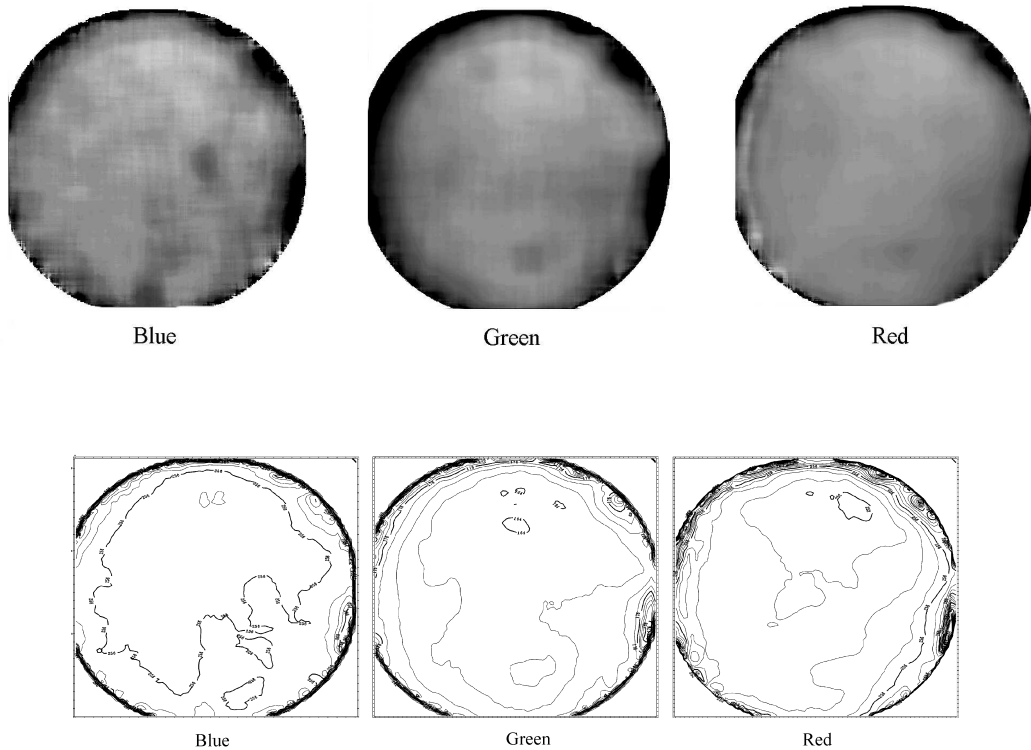


Fig. 8 Scans of filter V in blue, green and red light (upper panel) and their corresponding transmission contours (lower panel).

4 OBSERVATION ON THE TELESCOPE

The final estimate of the effects caused by inhomogeneities in the coating should be made through observing stars with the BFOSC on the telescope. Ideally, we should choose a sky region with standard stars uniformly distributed over the whole field covered by the CCD. Unfortunately, such sky regions do not exist at present. Therefore, our observation described below could tell something, but still not thoroughly, about the question we are concerned with. In December of 1999, we took two direct images, image d181 (exposure time 6 seconds) and image d182 (exposure time 10 seconds), of the open star cluster M67, using the 2.16-m telescope + BFOSC + V-filter. By aperture photometry and by comparison with the CCD photometry of M67 performed by Gilliland et al. (1991), we found 100 common stars. Removing 11 known variables, we finally had 89 stars for a final comparison with the Gilliland et al. results (these 89 stars are not uniformly distributed over the whole field of view, and so the present test cannot check the inhomogeneities everywhere on the filter). The results are given in Fig. 9. In order to show that these are not due to errors in measurements, we also give in Fig.10 the magnitude difference obtained from the two exposures d181 and d182 which were taken successively in time with the star images shifted by about 2 pixels on the CCD. It can be seen that, from the brighter to the fainter end, the scatter of the points increases as the input S/N-ratio decreases. However, the scatter at the bright end is very small, and these same stars measured on d181 show a much larger scatter as compared with Gilliland et al.'s measurements with rms error in V of 0.018 mag (Fig. 9). Here, the influence caused by the difference between the two photometric systems should be very small because, for the V band, the V magnitude of BFOSC is close to the standard V system (the results will be published elsewhere).

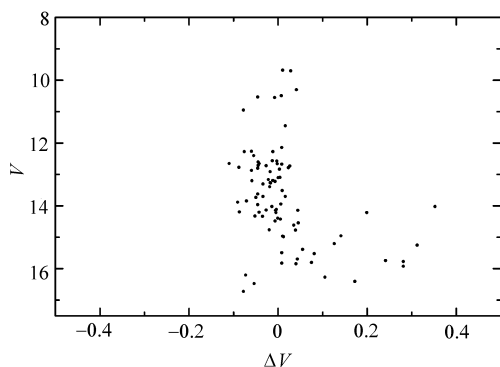


Fig. 9 Magnitude difference between the exposure d181 and that of Gilliland et al. (1999).

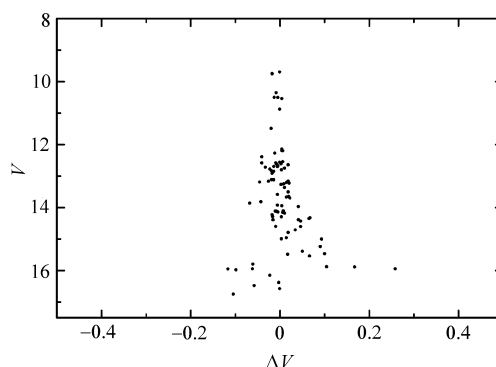


Fig. 10 Magnitude difference between exposures d181 and d182.

5 CONCLUDING REMARKS

Although the method of our test was not perfect, we have definitely established that the spectral transmission curves of the existing BFOSC coated filters varies with the position on the

filter. These variations cannot be removed by flat-field corrections except for the narrow-band filters. The seriousness of the effects caused by such variations on astronomical photometry depends on the accuracy required by the research programs.

For the studies of variable stars with amplitudes less than 0.05 magnitudes, or studies aiming at establishing accurate C-M diagrams of star clusters, we recommend using usual Schott glass filters of Bessell's prescription without anti-reflection coatings. Although existing coated filters can reach, for the same exposure time, fainter magnitudes, they lose accuracy even at the bright end.

References

- Bessell N. S., 1990, *PASP*, 102, 1181
Gilliland R. L., et al., 1991, *AJ*, 101,541
King I. R., 1986, *Data Analysis in Astronomy II*
Stetson P. B., 2000, *PASP*, 112, 925
Yao B., Zhang C., Li Q., 2002, *Pub. of Purple Mountain Observatory*, in press